Dielectric Loaded Substrate Integrated Waveguide (SIW) H-Plane Horn Antennas

Hao Wang, *Member, IEEE*, Da-Gang Fang, *Fellow, IEEE*, Bing Zhang, and Wen-Quan Che, *Member, IEEE*

***Abstract*—A dielectric loaded substrate integrated waveguide (SIW) H-plane sectoral horn antenna has been proposed in this paper. The horn and the loaded dielectric are integrated by using the same single substrate resulting in easy fabrication and low cost. Two antennas with rectangular and elliptical shaped loaded dielectrics were designed and fabricated. These antennas have high gain and narrow beamwidths both in the E-plane and in the H-plane. The results from the simulation and those from the measurement are in good agreement. To demonstrate applications of the array, the small aperture elliptical dielectric loaded antenna has been used to form an array to obtain higher gain and to form a one-dimensional monopulse antenna array.**

***Index Terms*—Array, dielectric loaded, H-plane sectoral horn, substrate integrated waveguide.**

I. Introduction

THE rectangular waveguide horn is one of the simplest and probably the most widely used microwave antenna. Recently, the substrate-integrated waveguide (SIW) technique has been investigated and developed to construct the planar rectangular waveguide [1]–[9]. The application of SIW for the design of an integrated H-plane sectoral horn antenna was proposed in [10]. This structure is easy to be integrated with the feed network and is a good candidate to feed the surface-wave antennas or the leaky-wave antennas [11]. On the other hand, the patch fed planar dielectric slab extended hemi-elliptical lens antenna was reported in [12]. The SIW millimeter-wave monopulse antenna was introduced in [13].

In this paper, we present a dielectric loaded H-plane sectoral SIW horn antenna. This antenna is integrated by using a single substrate. It is easy to fabricate and the structure is compact. To eliminate the higher order modes in the waveguide, the thickness of the substrate is restricted. The loaded dielectric slab in front of the horn aperture can be considered as a dielectric guiding structure excited by the horn aperture resulting in a narrower beamwidth in the E-plane. For a horn of maximum gain, the aperture phase distribution along the H-plane is nearly uniform without the dielectric loading. If the length of the slab is not properly chosen the beamwidth in the H-plane will be broadened. To reduce the size, the length of the horn can be shortened, but the quadratic phase error will increase simultaneously. In this case, the dielectric loading may serve as the phase corrector in the H-plane. Through proper choosing of the length of the dielectric slab, both of the beamwidths in the E-plane and in the H-plane will be narrowed and consequently the high gain is obtained. The good agreement between the simulated results and those from experiments confirms the correctness of the proposed idea and the advantage of this horn antenna. In addition, in this paper the single horn is also used to form a high gain array and a one-dimensional monopulse array.

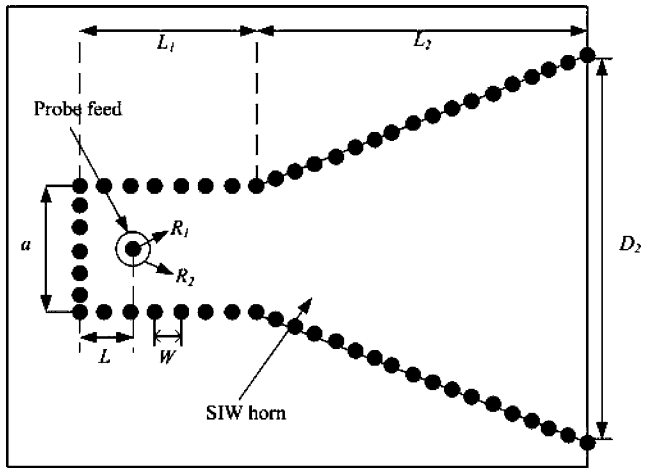

Fig. 1. Geometry of SIW horn antenna without dielectric loading. $W = 1$ mm, $L = 1.8$ mm, $a = 5$ mm, $D_2 = 14$ mm, $L_1 = 7$ mm, $L_2 = 15$ mm, $R_1 = 0.25$ mm, $R_2 = 0.5$ mm.

In this paper, a substrate with dielectric constant ϵ_r of 4.8, thickness b of 2.5 mm and a working frequency of 27 GHz are used in all the simulated and measured results. All the simulated results are gotten from Ansoft HFSS.

II. SIW H-Plane Sectoral Horn Antenna Without Dielectric Loading

The geometry of the SIW H-plane sectoral horn antenna is given in Fig. 1. The rectangular waveguide and sectoral horn antenna are integrated by using the same single substrate based on the SIW technology. As a result they are easy to fabricate and the structure is compact. In the waveguide of the SIW horn, the dominant mode is TE_{10}. To ensure the single mode excitation of the horn, the width a' and the thickness b' should be chosen based on the inequality:$2a' > \lambda/\sqrt{(\epsilon_r)} > \max(a', b')$. The given dielectric constant and the thickness of the substrate

Manuscript received January 24, 2009; revised July 11, 2009. First published December 28, 2009; current version published March 03, 2010. This work was supported in part by the Nature Science Foundation of China under Grant 60671038 and in part by the Key Laboratory of Target Detection at NJUST.

H. Wang, D.-G. Fang, and W.-Q. Che are with the Department of Communication Engineering, Nanjing University of Science and Technology, Nanjing 210094, China (e-mail: fangdg@mail.njust.edu.cn).

B. Zhang was with the Department of Communication Engineering, Nanjing University of Science and Technology, Nanjing 210094, China. He is now with ZTE Company, Shenzhen 51805, China.

Color versions of one or more of the figures in this paper are available online at http://ieeexplore.ieee.org.

Digital Object Identifier 10.1109/TAP.2009.2039298

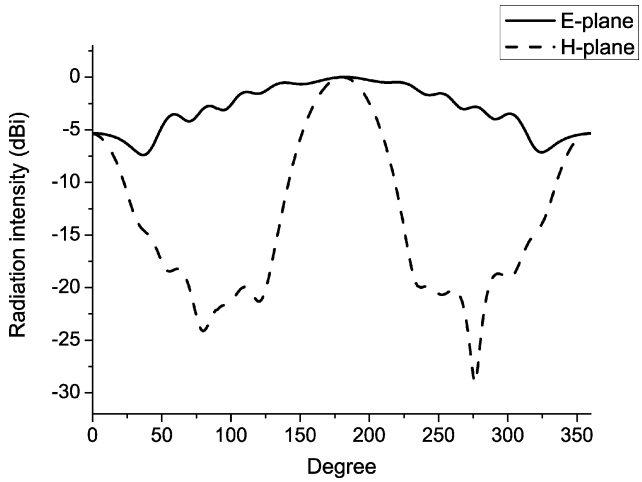

Fig. 2. Radiation patterns of SIW horn antenna shown in Fig. 1.

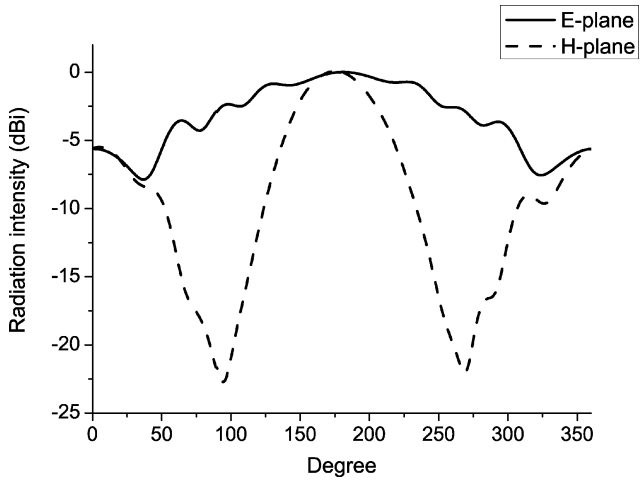

Fig. 3. Radiation patterns of shortened length SIW horn antenna without dielectric loading.

satisfy the inequality. The equivalent width a of the SIW has been derived in [14] as

$$a = \frac{2a'}{\pi} ctg^{-1}\left(\frac{\pi W}{4a'} \ln \frac{W}{4R}\right) \tag{1}$$

where W is the spacing between two adjacent vias, and R is the radius of the via. Based on the design rule of SIW, R and W are chosen to be 0.8 mm and 1 mm [14]. From formula (1), the width a of SIW is determined as 5 mm. The equivalent thickness b of the SIW is equal to the the thickness of the waveguide b'. For a given aperture $D_2 = 14$ mm, it was found that the length of the horn L_2 affects not only the quadratic phase error on aperture along the H-plane but also the higher order mode excitation in the horn. A reasonable length of 15 mm was determined to obtain the acceptable quadratic phase error and single mode on the aperture. The simulated gain and side lobe level are 6.73 dBi and -12.08 dB; the simulated beamwidths of the E-plane and the H-plane are 180° and 48° respectively. The simulated radiation patterns are shown in Fig. 2.

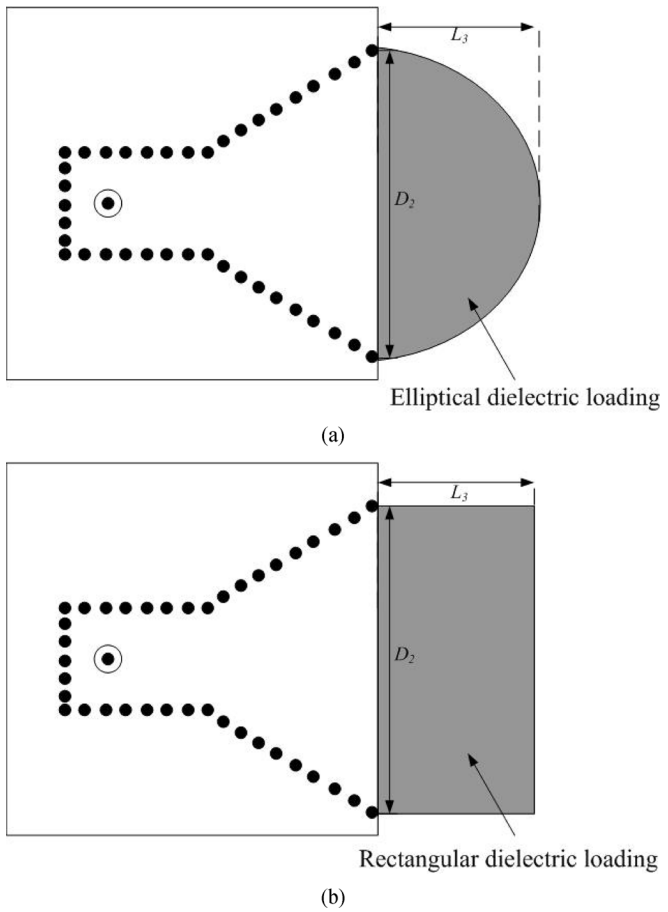

Fig. 4. Dielectric loaded SIW horn antennas. (a) Elliptical dielectric loading. (b) Rectangular dielectric loading.

III. Dielectric Loaded SIW H-Plane Horn Antennas

The beamwidth in the H-plane can be controlled through the aperture size in the H-plane. The beamwidth in the E-plane is determined by the aperture size in the E-plane that is limited. In some applications, a narrow beamwidth in the E-plane is also desired. For this purpose, a dielectric slab is placed in front of the aperture of the horn. This slab serves as the dielectric guiding structure in the E-plane. In the H-plane, for a horn with maximum gain, the aperture phase distribution along the H-plane is nearly uniform without the dielectric loading. If the length of the slab is not properly chosen the beamwidth in the H-plane will even be broadened. Take the example of the horn in Fig. 1. If it is loaded by a dielectric elliptical slab with a length of 1.4 mm, the beamwidth in the H-plane is broadened by 18°. The dielectric loading was used in the H-plane sectoral shortened length horn antenna to reduce the size long before [11]. In this case, the dielectric loading serves as the phase corrector in the H-plane to compensate the quadratic phase error caused from the shortened length. Through proper choosing of the length of the dielectric slab, both of the beamwidths in the E-plane and in the H-plane will be narrowed and consequently the high gain is obtained.

Now we change the length L_2 in Fig. 1 from 15 mm to 10 mm. The simulated radiation patterns of this H-plane

TABLE I
COMPARISON OF THE COMPUTING TIME USED USING THE DIFFERENT METHODS.

	Gain(dBi)	Beamwidth in E-plane (degree)	Beamwidth in H-plane (degree)	Sidelobe Side lobe levels (dB)
Hyperbola	10.33	62	44	-9.25
Parabola	10.95	68	46	-9.82
Ellipse	11.40	60	42	-10.03
Rectangle	11.68	58	40	-8.27

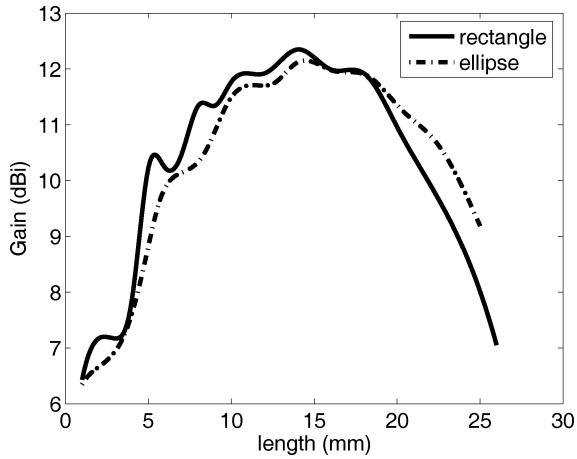

Fig. 5. Gains versus the length of loaded dielectric.

horn antenna without dielectric sector are shown in Fig. 3. The gain is 5.75 dBi, the back sidelobe level is 11.78 dB and the beamwidths of the E- and H-plane are 178° and 63°, respectively. An elliptical dielectric slab and a rectangular dielectric slab are now placed in front of the aperture of the horn, respectively. The corresponding structures are shown in Fig. 4. The gains versus the lengths of dielectric slabs are shown in Fig. 5. The variations of beamwidths in the E-plane and in the H-plane are given in Fig. 6. From these figures, it is seen that on the whole, the beamwidths monotonically decrease with the increase of the dielectric length. For example, when the length of elliptical slab is 9.8 mm, the gain is 11.68 dBi and the beamwidths in the E-plane and in the H-plane are 60° and 42°. When comparing with the SIW antenna without dielectric loading, the gain has increased by 5.93 dB and the beamwidths in the E-plane and in the H-plane have reduced by 118° and 21°, respectively. The side lobe levels versus the length of dielectric loading are shown in Fig. 7.

Furthermore, different shapes of dielectric loading were investigated. They are ellipse, rectangle, hyperbola and parabola. Table I shows the results. From these results, it is seen that the rectangular slab gives the narrowest beamwidths in both E- and H-planes and the highest gain with slightly higher side lobe level.

The rectangular and elliptical dielectric loaded SIW horn antennas were fabricated and measured. The length of dielectric slab is 9.8 mm. An SMA probe was used to feed the antenna. The photos of antennas are given in Fig. 8. The simulated and measured S11 are given in Fig. 9. The E- and H- plane radiation patterns of rectangular dielectric loaded SIW horn antenna

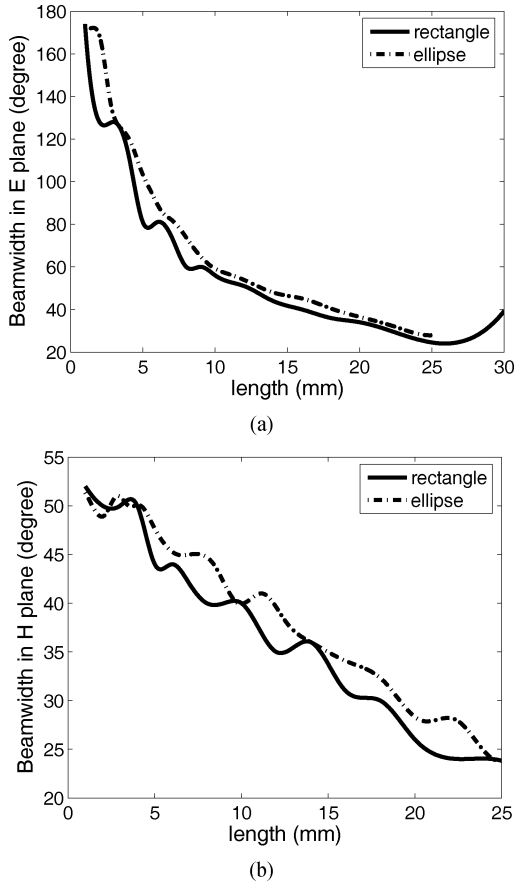

Fig. 6. Beamwidths versus the length of loaded dielectric. (a) E plane. (b) H plane.

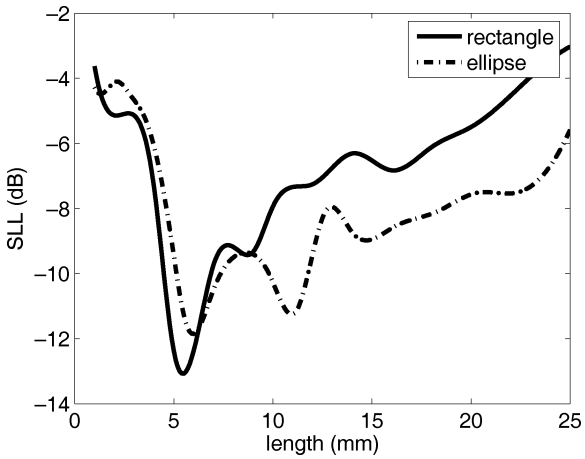

Fig. 7. Side lobe levels versus the length of loaded dielectric.

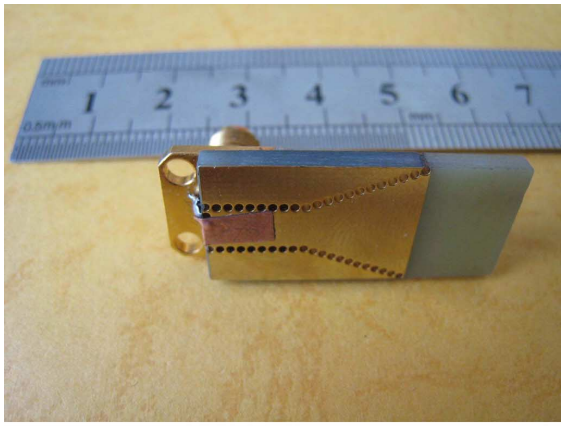

(a)

(b)

Fig. 8. Two kinds of SIW sectoral horn antennas. (a) Rectangular loading. (b) Elliptical loading.

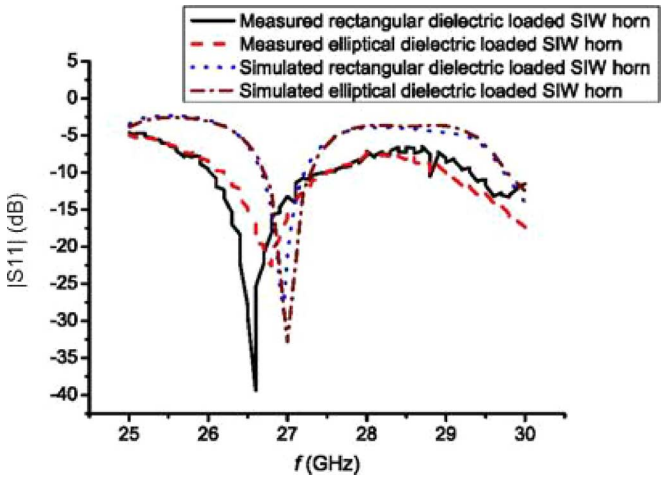

Fig. 9. Simulated and measured $|S11|$ parameters.

are shown in Fig. 10. The measured gain is 9.7 dBi. The corresponding simulated and measured radiation patterns of elliptical dielectric loaded SIW horn antenna are given in the Fig. 11. The measured gain is 9.3 dBi. The results from the simulation and those from measurement are in good agreement.

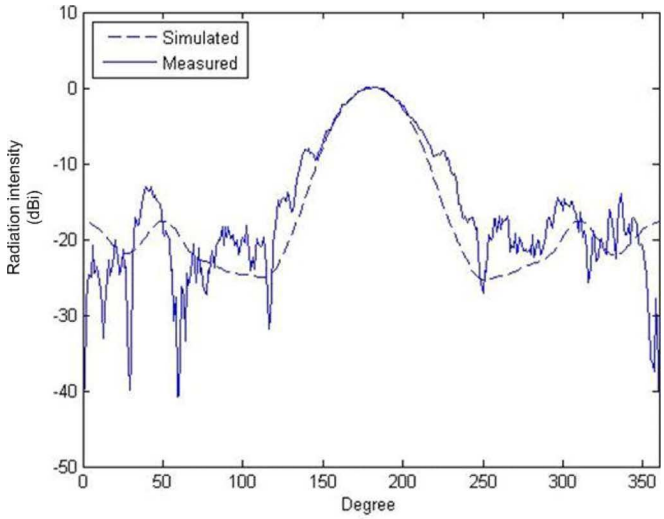

(a)

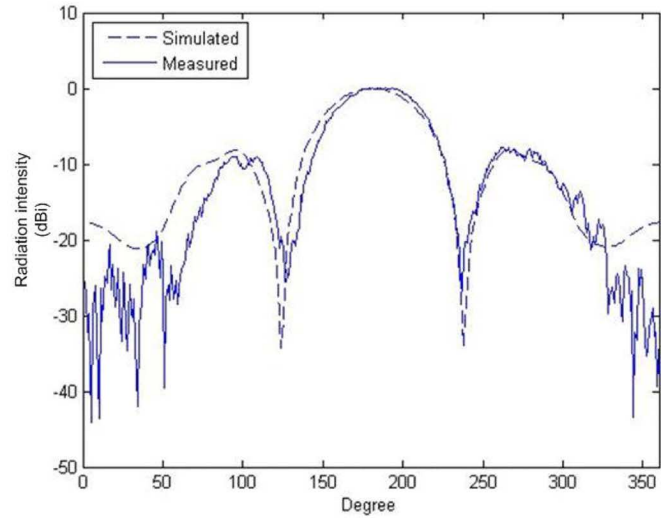

(b)

Fig. 10. Radiation patterns of rectangular dielectric loaded SIW horn antenna. (a) H plane. (b) E plane.

IV. SIW Antenna Array

To construct the antenna array in H-plane, the aperture of SIW H-plane horn antenna should be within one wavelength in H-plane. The dielectric loaded small aperture SIW H-plane horn antenna is introduced for such purpose. The size of the aperture is 10 mm which is less than one wavelength. The simulated results are given when the length of dielectric slab is 7 mm. The gain is 8.83 dBi and the beamwidths of the E- and H-plane are 80° and 60°. This dielectric loaded small aperture SIW antenna was also fabricated. The photo is given in Fig. 12. The simulated and measured reflection coefficients are shown in Fig. 13, while the simulated and measured radiation patterns are illustrated in Fig. 14. The measured gain is 9.1 dBi.

A SIW antenna array formed by four small aperture SIW elements is shown in Fig. 15. As we can see, this dielectric loaded SIW horn element can be integrated in the array easily. The detailed dimensions of the 5-way power divider are also shown in the figure. The photo of this array is given in Fig. 16. The simulated and measured $|S11|$ of SIW antenna array are shown in

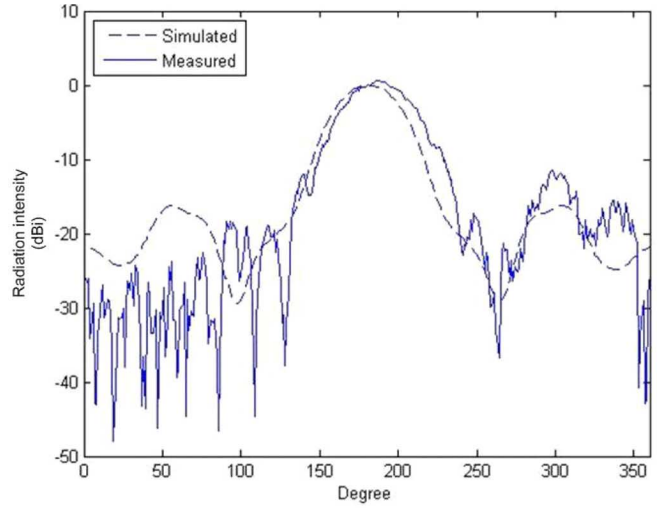

(a)

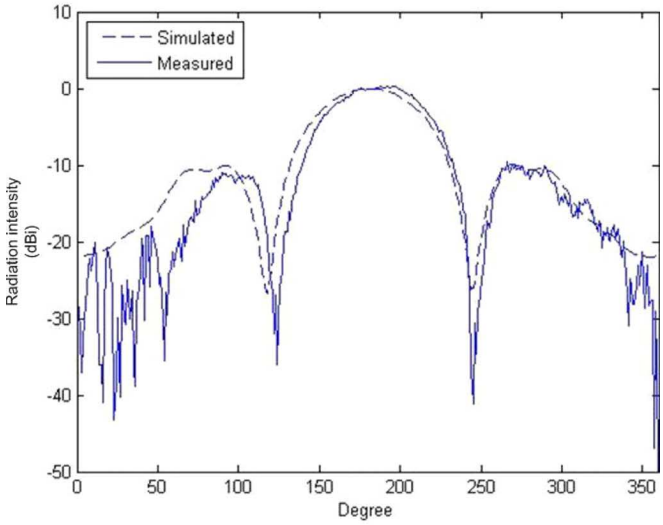

(b)

Fig. 11. Radiation patterns of elliptical dielectric loaded SIW horn antenna. (a) H plane. (b) E plane.

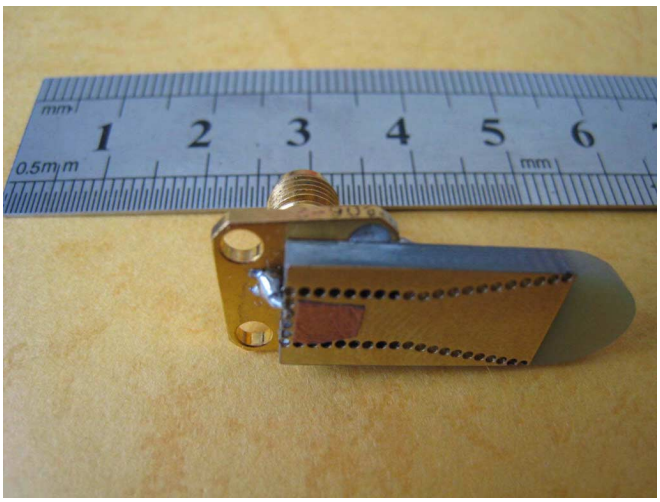

Fig. 12. Elliptical dielectric loaded small aperture SIW horn antenna.

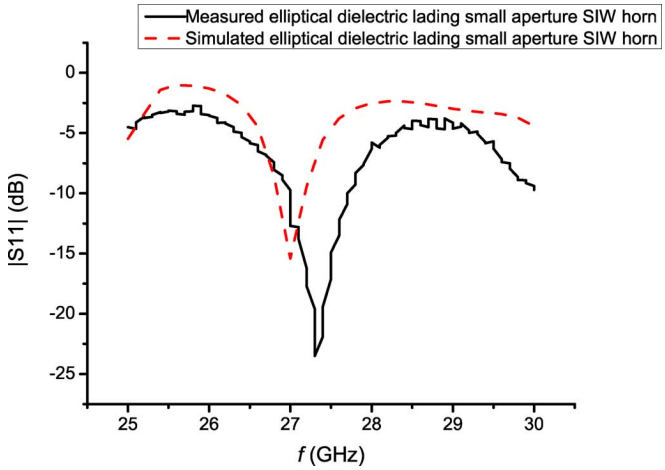

Fig. 13. Simulated and measured $|S11|$ of elliptical dielectric loaded small aperture horn.

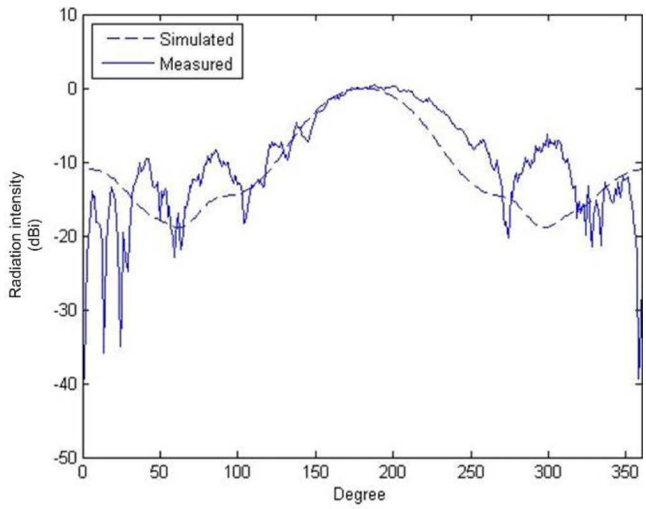

(a)

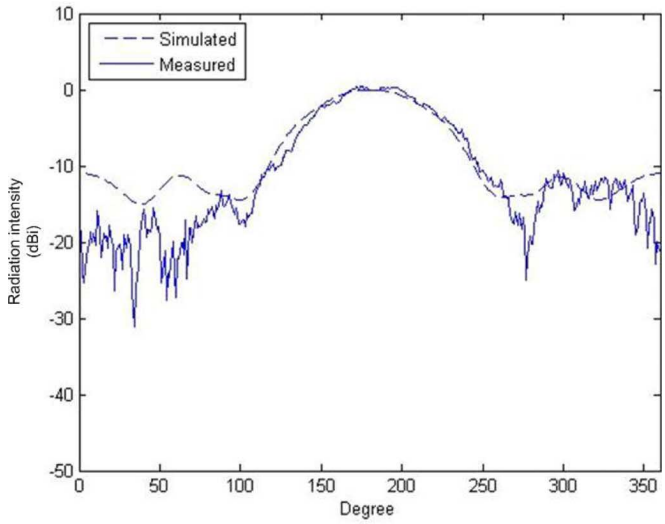

(b)

Fig. 14. Radiation patterns of elliptical dielectric loaded small aperture SIW horn antenna. (a) H plane. (b)E plane.

Fig. 17. The bandwidth (VSWR $\leq$ 2) is 1.5% at the central frequency 27 GHz from the simulated results. The measured $|S11|$ curve is shifted to the low frequency due to the fabrication error. The corresponding radiation patterns of the array are

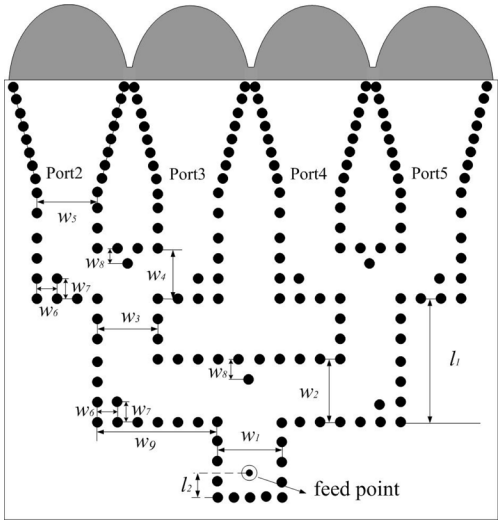

Fig. 15. Structure of 1×4 dielectric loaded SIW antenna array. $w_1 = w_2 = w_3 = w_4 = 4.5$ mm, $w_5 = 5$ mm, $w_6 = w_7 = 1.5$ mm, $w_8 = 1.1$ mm, $w_9 = 10$ mm, $l_1 = 12$ mm, $l_2 = 1.5$ mm.

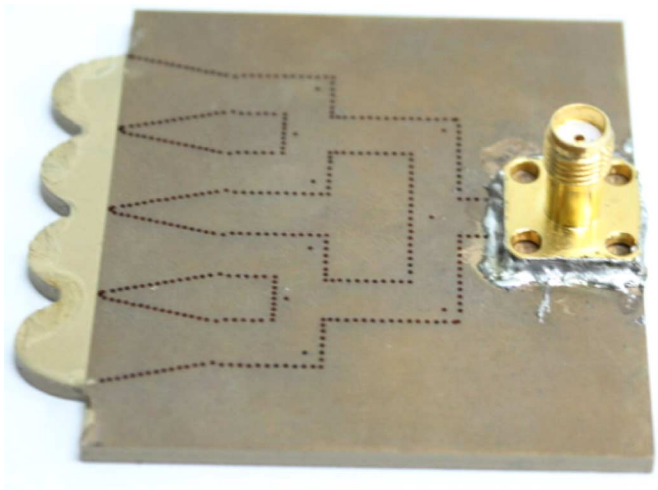

Fig. 16. Photo of 1×4 dielectric loaded SIW antenna array.

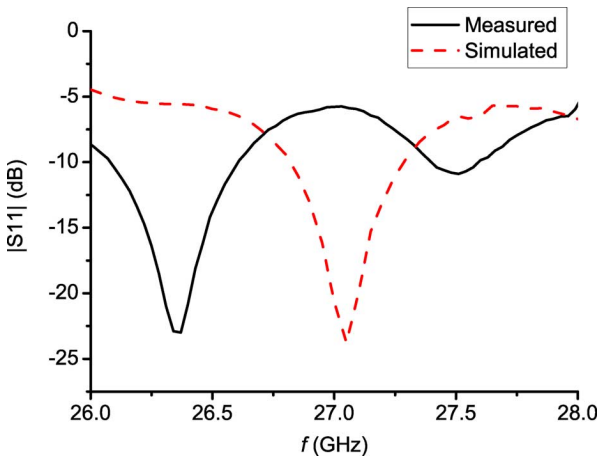

Fig. 17. Simulated and measured $|\mathrm{S}11|$ of 1×4 SIW antenna array.

shown in Fig. 18. The simulated gain of the array is 14.9 dBi. The beamwidths are 76° in the E plane and 14° in the H plane, respectively. The measured gain is 13.75 dBi. Furthermore, a

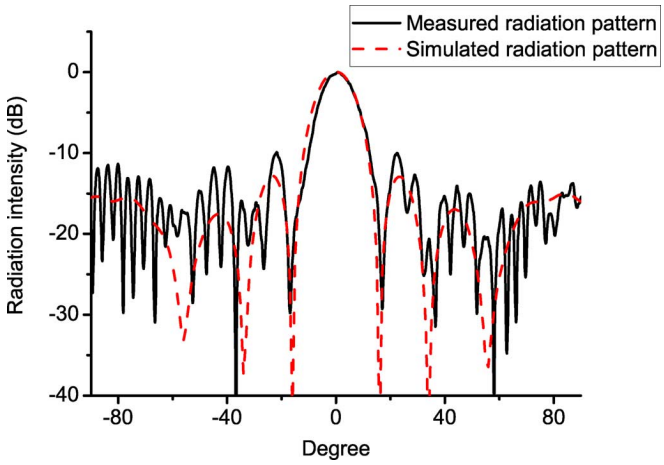

Fig. 18. Radiation patterns of 1×4 SIW antenna array.

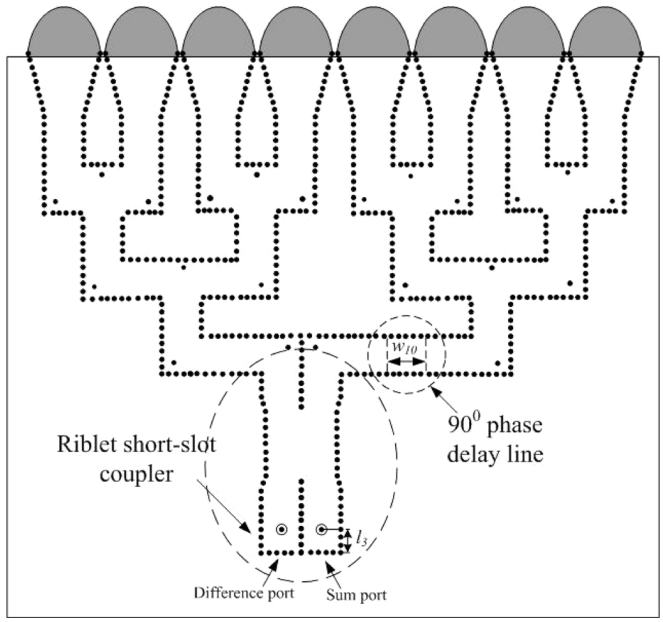

Fig. 19. Structure of monopulse dielectric loaded SIW antenna array. $l_3 = 1.5$ mm, $w_{10} = 1.6$ mm.

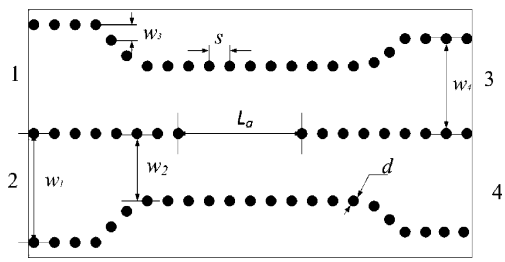

Fig. 20. Structure of Riblet short-slot coupler. $d = 0.4$ mm, $s = 0.8$ mm, $w_1 = 4.5$ mm, $w_2 = w_4 = 3.9$ mm, $w_3 = 0.175$ mm, $L_a = 6.5$ mm.

one-dimensional SIW monopulse antenna array was developed. The structure of this monopulse array given in Fig. 19 is very compact and simple. This monopulse antenna array is formed by two 1×4 sub-arrays. A Riblet short-slot coupler [15] and 90° phase delay line are used to form a comparator. The detailed dimensions of the Riblet short-slot coupler are shown in

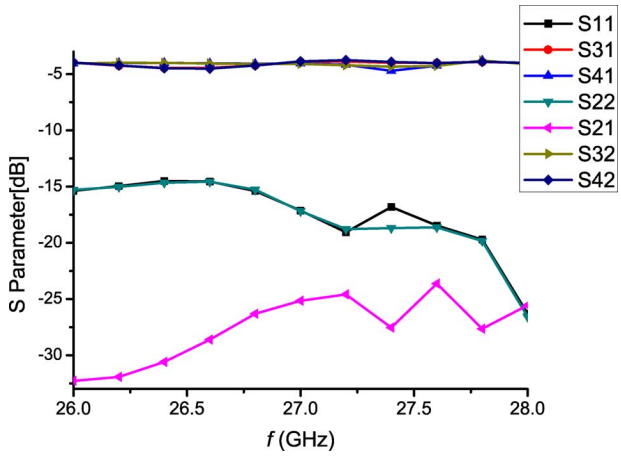

Fig. 21. Magnitude of simulated S parameters of Riblet short-slot coupler.

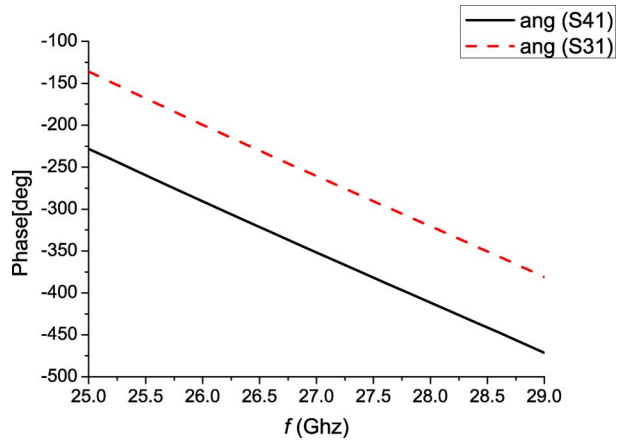

Fig. 22. Phase of simulated S parameters of Riblet short-slot coupler.

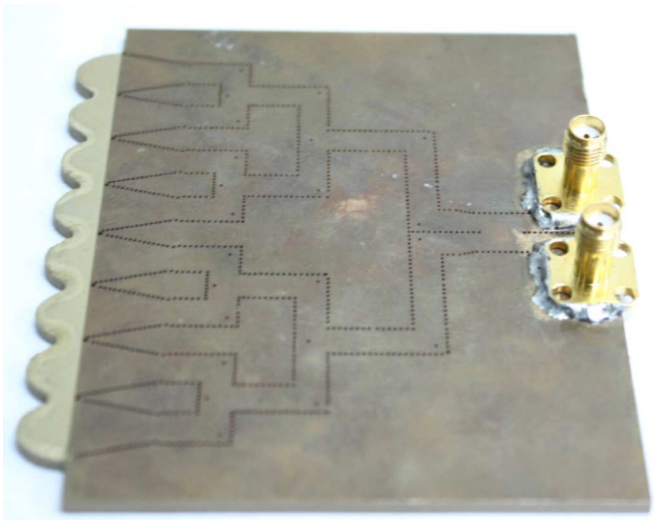

Fig. 23. Photo of 1 × 8 dielectric loaded SIW monopulse antenna array.

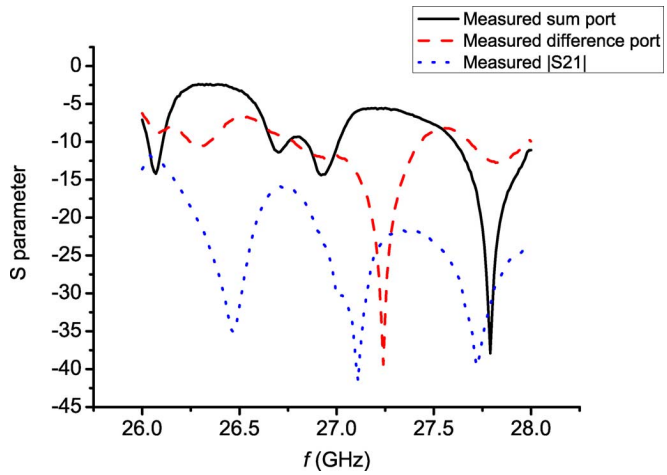

Fig. 24. Measured S parameters of monopulse SIW horn antenna.

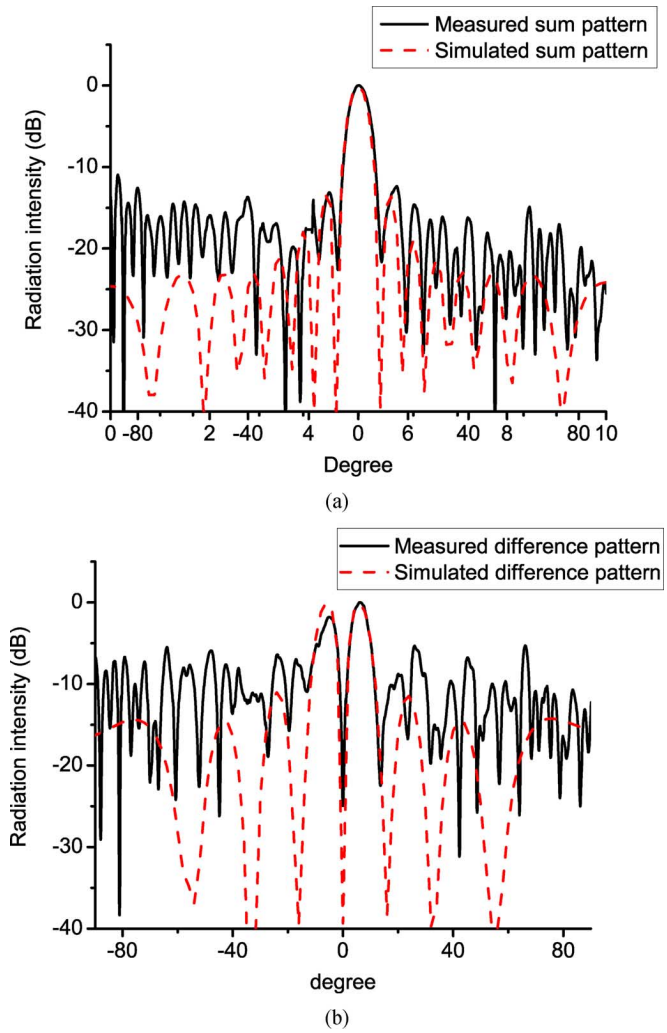

Fig. 25. Sum and difference radiation patterns of monopulse SIW horn antenna. (a) Sum pattern. (b) Difference pattern.

Fig. 20. The simulated S parameters of coupler are shown in Figs. 21–22. From the simulated results, it is shown that at the frequency of 27 GHz, the phase difference between coupled and direct signals is $-90 \pm 1.5°$. Isolation and return loss for this coupler are around -20 dB. The photo of this monopulse array is given in Fig. 23. The measured S parameters of the array are shown in Fig. 24. The isolation between two ports is -30 dB at the resonant frequency 27 GHz. The simulated and measured sum and difference patterns of monopulse SIW array are shown in Fig. 25. The simulated gain and the side lobe level of sum pattern are 17.9 dBi and 9.63 dB, respectively. The measured gain

is 15.65 dBi. The big difference between simulated result and the measured one is believed to be the dielectric loss especially in the case of using the long feed line to form a large array. In the above simulation, the dielectric loss tangent is assumed to be 0.001 according to the company's data sheet measured at X band. In Ka band the loss tangent will be much larger. As an evidence, if we choose the loss tangent to be 0.003, the gain of the monopulse array reduces to 15.3 dBi that is very closer to the measured gain. The simulated and measured null depths of difference pattern are -39 dB and -25 dB, respectively.

V. Conclusion

This paper presents the optimized design of dielectric loaded substrate integrated waveguide H-plane antennas. Through proper choosing of the structure and the parameters, the maximum gain for the given size or the minimum size for a given gain may be achieved. The reasonable agreement between the simulated results and the experimental ones verifies the correctness of the designs. In addition, the examples of two arrays show the potentiality of the proposed antenna for many applications.

Acknowledgment

The authors would like to thank the reviewers for their constructive comments and their scrutiny in correcting the errors in this paper.

References

[1] D. Deslandes and K. Wu, "Integrated transition of coplanar to rectangular waveguides," in *IEEE MTT-S Int. Microwave Symp. Dig.*, Feb. 2001, pp. 619–622.

[2] Y. Cassivi *et al.*, "Dispersion characteristics of substrate integrated rectangular waveguide," *IEEE Microw. Wireless Compon. Lett.*, vol. 12, no. 9, pp. 333–335, 2002.

[3] C.-H. Tseng and T.-H. Chu, "Measurement of frequency-dependent equivalent width of substrate integrated waveguide," *IEEE Trans. Microw. Theory Tech.*, vol. 54, no. 4, pp. 1431–1437, 2006.

[4] F. Xu and K. Wu, "Guided-wave and leakage characteristics of substrate integrated waveguide," *IEEE Trans. Microw. Theory Tech.*, vol. 53, no. 1, pp. 66–73, 2005.

[5] D. Deslande and K. Wu, "Single-substrate integration technique ofplanar circuits and waveguide filters," *IEEE Trans. Microw. Theory Tech.*, vol. 51, no. 2, pp. 593–596, 2003.

[6] A. Zeid and H. Baudrand, "Electromagnetic scattering by metallic holes and its applications in microwave circuit design," *IEEE Trans. Microw. Theory Tech.*, vol. 50, no. 4, pp. 1198–1206, 2002.

[7] L. Yan *et al.*, "Simulation and experiment on SIW slot array antenna," *IEEE Microw. Wireless Compon. Lett.*, vol. 14, no. 9, pp. 446–448, 2004.

[8] D. Deslandes and K. Wu, "Integrated microstrip and rectangular waveguide in planar form," *IEEE Microw. Wireless Compon. Lett.*, vol. 11, pp. 68–70, 2001.

[9] F. Xu, K. Wu, and W. Hong, "Domain-decomposition FDTD algorithm combined with numerical TL calibration technique and its application in parameter extraction of substrate integrated," *IEEE Trans. Microw. Theory Tech.*, vol. 54, no. 1, pp. 329–338, 2006.

[10] Z. L. Li and K. Wu, "An new approach to integrated horn antenna," in *Proc. Int. Symp. on Antenna Technology and Applied Electromagnetics*, Jul. 2004, pp. 535–538.

[11] R. E. Collin and F. J. Zucker, *Antenna Theory, Part 2*. New York: McGraw-Hill, 1969.

[12] L. Xue and V. Fusco, "Patch fed planar dielectric slab extended hemielliptical lens antenna," *IEEE Trans. Antennas Propag.*, vol. 56, no. 3, pp. 661–666, 2008.

[13] Y. J. Cheng, W. Hong, and K. Wu, "Design of a monopulse antenna using a dual V-type linearly tapered slot antenna (DVLTSA)," *IEEE Trans. Antennas Propag.*, vol. 56, no. 9, pp. 2903–2906, 2008.

[14] W. Che, K. Deng, D. Wang, and Y. L. Chow, "Analytical equivalence between substrate-integrated waveguide and rectangular waveguide," *IET Microw. Antennas Propag.*, vol. 2, no. 1, pp. 35–41, 2008.

[15] D. M. Pozar, *Microwave Engineering*, 2nd ed. New York: Wiley, 1998.

Hao Wang (M'08) received the B.E. and Ph.D. degrees from the Nanjing University of Science and Technology (NJUST), Nanjing, China, in 2002 and 2009.

He is currently a Lecturer at the NUST. His research is focused on microstrip antennas and related electromagnetic simulation.

Da-Gang Fang (SM'90–F'03) was born in Shanghai, China. He graduated from the graduate school of Beijing Institute of Posts and Telecommunications, Beijing, China, in 1966.

From 1980 to 1982, he was a Visiting Scholar at Laval University (Quebec, Canada), and the University of Waterloo (Ontario, Canada). Since 1986, he has been a Professor at the Nanjing University of Science and Technology (NJUST), Nanjing, China. Since 1987, he had been a Visiting Professor with six universities in Canada and in Hong Kong. He has authored and coauthored three books, two book chapters and more than 380 papers. He is also the owner of three patents. His research interests include computational electromagnetics, microwave integrated circuits and antennas and EM scattering.

Prof. Fang is a Fellow of the Chinese Institute of Electronics (CIE). He was the recipient of the National Outstanding Teacher Award and People's Teacher Medal, and the Provincial Outstanding Teacher Award. He is an Associate Editor of two Chinese journals and is on the Editorial or Reviewer Board of several international and Chinese journals. He was TPC Chair of ICMC 1992, Vice General Chair of PIERS 2004, the member of International Advisory Committee of six international conferences and TPC Co-Chair of APMC 2005 and is the General Co-Chair of ICMMT 2008. His name was listed in *Marquis Who is Who in the World* (1995) and in *International Biographical Association Directory* (1995)

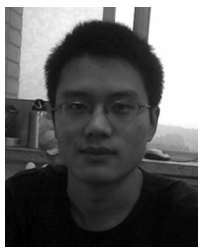

Bing Zhang received the B.S. and M.S. degrees in electrical engineering from Nanjing University of Science and Technology, Nanjing, China, in 2007 and 2009, respectively.

Now, he is working at the ZTE Company, Shenzhen, China.

Wen-Quan Che (M'01) received the B.Sc. degree from the East China Institute of Science and Technology, China, in 1990, the M.Sc. degree from the Nanjing University of Science and Technology (NJUST), China, in 1995; and the Ph.D. degree from City University of Hong Kong (CITYU), in 2003.

In 1999, she was a Research Assistant at CITYU. From March 2002 to September 2002, she was a Visiting Scholar at the Polytechnique de Montreal, Canada. She is currently a Professor in NJUST. In 2007–2008, she conducted the academic research with the Institute of HFT, Technische University Munchen. Her interests include electromagnetic computation, planar/co-planar circuits and subsystems in RF/microwave frequency. She has authored or coauthored over 70 articles in refereed journals.

Dr. Che was the recipient of the 2007 Humboldt Research Fellowship presented by the Alexander von Humboldt Foundation of Germany, and she was also the recipient of the 5th China Young Female Scientists Award in 2008.